ASSESSING THE ELECTROCHEMICAL BEHAVIOR OF FERRITIC FeCrAl ALLOYS IN HIGH TEMPERATURE WATER

R. B. REBAK, T. B. JUREWICZ, E. J. DOLLEY
GE Global Research
1 Research Circle, Schenectady, NY 12309, USA

ABSTRACT

Zirconium alloys have been used successfully as cladding for urania fuel for over six decades for the production of electricity. However, since the tsunami induced Fukushima accident of March 2011, there is a concerted decision to look for materials which are less reactive with steam at T > 1000°C when there is no coolant. One alternative is to use iron-chromium-aluminum (FeCrAl) alloys such as APMT, C26M, ODS FeCrAl, etc. This concept is being proposed in several countries and it is the main driving concept by General Electric and Oak Ridge National Laboratory in the US. Ferritic FeCrAl alloys have never been used before to manufacture internal components in a light water power reactor. Therefore, the behavior of FeCrAl needs to be appropriately measured against the behavior of materials which are known to perform efficiently and are currently in use. The objective of the current work was to assess the aqueous high temperature electrochemistry of C26M and APMT (named IronClad) in parallel to other alloys such as Zircaloy-2, X-750 and 304SS. Measurements were conducted in high purity water and in water contaminated with zinc nitrate and zinc acetate. Results show that IronClad react to the reactor environment in the same manner as the familiar austenitic alloys 304SS and X-750. This is because IronClad and the well-known austenitic alloys form a protective film of chromia on the surface exposed to the coolant, and therefore react electrochemically in a similar manner to the environment.

Introduction

Electricity generated using nuclear energy has been around for six decades. The materials used to build commercial nuclear power plants have not changed significantly in this time [1]. Light water reactors use nuclear energy to make steam at a temperature near 300°C. The main construction material for reactors are carbon steels, austenitic stainless steels and nickel based alloys. The metallic cladding for the fuel (urania) was in general a zirconium based alloy. Zirconium and its alloys were selected mainly because they have a transparency to thermal neutrons approximately ten times higher than for stainless steels. The composition of the zirconium alloys evolved in time for over six decades, mainly to make them more resistant to corrosion in 300°C water. Zirconium is not resistant to attack by steam at temperatures higher than 600-800°C.

In the Fukushima Daiichi accident of March of 2011, the plant black out caused a lack of active cooling in the reactor core, and therefore zirconium reacted with water and steam to produce large amounts of hydrogen gas and heat. The ignition of hydrogen was shown live all around the globe. Since then, the international materials community has been engaged to finding a safer alternative to the pair zirconium/urania for fuel [2]. The newer nuclear fuels are called Accident Tolerant Fuels (ATF) or Advanced Technology Fuel (ATF). Worldwide the efforts are focused in two main areas, (a) newer cladding for fuel, and (b) newer fuel [1]. Considerable effort is being invested in an accelerated characterization program of the newer ATF materials to evaluate their strengths and shortcomings for application to the current fleet of light water reactors. The evaluation areas and metrics

include determining performance not only for accident conditions but also for under normal operation conditions and for the end of fuel cycle (spent fuel disposition) [3]. General Electric and its partners including Oak Ridge National Laboratory have proposed using IronClad for the tubes containing the urania fuel pellets [2,4]. IronClad are ferritic iron-chromium-aluminum (FeCrAl) alloys which remain passive by the formation of a chromium oxide on the surface under normal operation condition and develop a protective alumina film on the surface under accident conditions [5].

The water or coolant inside of pressurized water reactors (PWR) and boiling water reactors (BWR) is generally at a temperature of near 300°C and may contain small addition of chemicals such a boric acid or lithium hydroxide to control fluence and pH of the water (PWR). Hydrogen gas is generally dissolved in the BWR and PWR waters to depress the corrosion potential of the metallic elements and minimizing corrosion. Other chemicals that may be added include soluble zinc, which was first implemented in BWR in the 1980s and in PWR starting in the mid-1990s. The mechanisms of how Zn provides benefits are still unclear, it may thin, densify and make more elastic the protective chromium oxide film on components, it may alter the electron and ionic transfer process, it may aid repassivation after protective oxide film rupture, etc. The addition of Zn also promotes dose reduction (decreases radiation build-up) by replacing cobalt in the oxides or crud accumulated on fuel rods. In general, it is now understood that Zn not only offers radioprotection but that a zinc conditioned oxide film mitigates all forms of corrosion in austenitic stainless steels and in nickel-based alloys [6,7,8,9]. The Zn may be injected at low concentrations (e.g.10 ppb) using highly soluble zinc acetate over extended periods of time (weeks to months) [9,10]. The beneficial effects of zinc may not show until after several months, since its action would be mostly controlled by diffusion processes in the surface oxide of the reactor cooling system (RCS).

The objective of the current work is to examine the electrochemical performance of IronClad FeCrAl cladding comparing to the performance of other classic materials like 304SS and X-750, which have been used in reactors for several decades (Table 1).

Table 1.
Nominal Compositions in mass percent of the studied materials

Element	Zircaloy-2 hcp	304SS austenitic	X-750 austenitic	C26M ferritic	APMT ferritic
Zr	~98	--	--	--	--
Fe	0.07-0.2	~70	7	~80	~70
Ni	0.03-0.08	8	~72	--	--
Cr	0.05-0.15	19	15	12	22
Al	--	--	0.7	6	5
Mo	--	--	--	2	3
Si	--	0.75 max	0.5 max	0.2	0.7 max
Mn	--	2 max	1 max	--	0.4 max
C	--	0.08 max	0.08 max	0.01 max	0.08 max
Other	1.5Sn	--	2.5Ti, 1Nb	0.05Y	Y, Hf

EXPERIMENTAL TECHNIQUE

The electrochemical measurements in pure water at 288°C and 10 MPa pressure were conducted in a 1-gallon (3.78 liter) stainless steel autoclave by controlling the water chemistry conditions at a water flow rate of 100 cm^3/min (Figure 1). The specimens for the electrochemical testing were cut in the form of strips 0.5 cm wide x 2.5 cm long and then

polished using a wet 600-grit emery paper. This geometry was required to fit the specimens through the autoclave top penetrations (Figure 2). All the test specimens were rinsed ultrasonically with high purity water.

The specimens for electrochemical measurements were spot welded to polytetrafluorethylene (PTFE) insulated stainless steel wires, which were mounted in a special fitting around the platinum counter electrode (Figure 2). Water in the loop was purified to 18 MΩ-cm through a demineralizer, an organic removal column, and a sub-micron filter before passing into a 1-gallon (3.78 liter) glass conditioning column. The water was equilibrated with appropriate mixtures of Ar, O_2, or H_2 to establish the desired water chemistry. Oxygen and hydrogen monitors were used for measuring the dissolved oxygen and hydrogen, respectively, in the inlet and outlet streams. The pH of high temperature pure water (near 300°C) is approximately 5.6.

The studied aqueous environments were simulated reactor environments with addition of only hydrogen or oxygen to high purity water without the addition of lithium or boron. The effect of zinc was studied by adding 100 ppm Zn^{2+} in the form of zinc nitrate ($Zn(NO_3)_2$) or zinc acetate ($Zn(CH_3COO)_2$). A platinum (Pt) electrode was used to monitor the effective redox potential of the electrolyte.

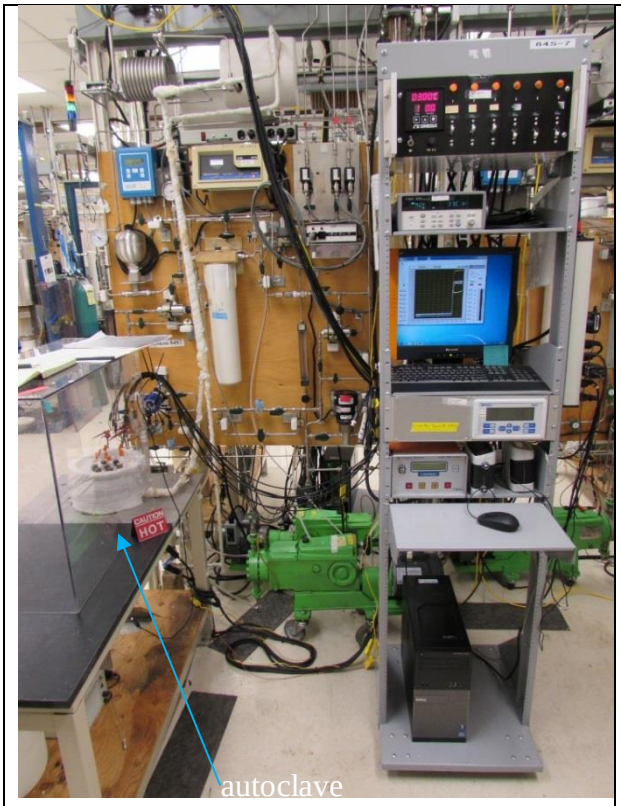

Figure 1. Recirculating autoclave system. The autoclave is at center left.

Figure 2. Six specimens mounted in the autoclave head. The Pt counter electrode is at the center

The materials used to manufacture the specimens for the electrochemical measurements (Table 1) were not cladding tubes or spacers but bars. The type of oxides formed on the specimens, which control the values of corrosion potential in the hydrogen or oxygen rich environments, depend mainly on the chemical composition of the alloys (Table 1) and have little or no correlation with other properties of the alloys such as grain size, and mechanical

strength. Except for zirconium, the other alloys in Table 1 will form a chromia rich oxide on the surface, providing the alloy with the benefits of passivity [5].

Electrochemical impedance spectroscopy and polarization resistance tests were performed according to ASTM G106 and G59/G102, respectively. Table 2 shows the density and the equivalent weights for the alloys studied (Table 1).

The polarization resistance tests, started at 20 mV below the corrosion potential (E_{corr}), applying a potentiodynamic rate of 0.167 mV/s, and ending at 20 mV above E_{corr}. The Polarization Resistance (R_p) is defined as the slope of the potential (E) vs. current density (i) at i = 0. The corrosion current density, i_{corr}, is related to the polarization resistance by the Stern –Geary coefficient B

$$R_p = \left(\frac{\partial \Delta E}{\partial i}\right) \; at \; i = 0, when \; \frac{\partial E}{\partial t} \rightarrow 0 \qquad (1)$$

$$i_{corr} = \frac{B}{R_p} \qquad (2)$$

where $$B = \frac{b_a \times b_c}{2.303(b_a + b_c)} \qquad (3)$$

b_a and b_c are the anodic and cathodic Tafel constants assumed to be 120 mV/decade. The corrosion rate can then be calculated using the Faraday equation

$$i_{corr}\left(\frac{\mu m}{y}\right) = \frac{k \times i_{corr} \times EW}{d} \qquad (4)$$

Where k is a conversion factor, and i_{corr} is the corrosion current density in A/cm² (calculated from the measurements of the resistance to polarization, R_p) (Eq. 2), EW is the equivalent weights for each the five alloys calculated according to ASTM G102, and d is the density (Table 2). The values of corrosion rate measured using the polarization resistance tests will be reported in the near future, when comparative mass change immersion corrosion tests results are concluded.

TABLE 2. Properties of the alloys.

	Zirc-2	**304SS**	**X-750**	**C26M**	**APMT**
d (g/cm³)	6.56	7.94	8.28	7.2	7.25
EW	22.8	25.1	26.5	23.2	22.5

EXPERIMENTAL RESULTS

Corrosion Potentials in 288°C water

Table 3 shows the timeline in 11 Steps of the electrochemical tests conducted over four months. Figure 3 shows the corrosion potential behavior for six weeks of five engineering alloys (Table 1) and platinum in pure water at 288°C.

The potential measurements were performed using a zirconia high temperature pH sensor with a Cu/Cu_2O internal junction as a reference electrode and an Agilent Model 34970A electrometer. The potential measurements were taken every 10 minutes. The measured potential values were converted to the normal hydrogen electrode (NHE) scale by the formula E_{NHE} (V) = $E_{Cu/Cu2O}$ (V) – 0.273. For the first 480 hours of immersion (Step 1) (Figure 3) the water contained dissolved hydrogen gas (300 ppb H_2), for the intermediate period of Step 2 (480-713 hours) the water contained dissolved oxygen gas (1000 ppb O_2). For the last period or Step 3 (713 h to 1000 h) the gas was again changed to 300 ppb hydrogen. Under hydrogen conditions the corrosion potential for the six materials was low and between -650 and -750 mV (NHE). The maximum separation between the corrosion potential for the six materials was generally in a band of less than 100 mV. At 480 h (20 days) of immersion the purging gas was changed from hydrogen to oxygen and a sudden increase of the corrosion potential for all the materials was observed (Figure 3). While in hydrogen atmosphere the potential of all the materials was approximately the same, under oxygen atmosphere there was a clear separation of the corrosion potential values. The highest (most noble) potential was for platinum and the lowest (least noble) was for Zircaloy-2. The potential of all the other materials including nickel-based X-750, austenitic stainless-steel type 304, and the two newer ferritic FeCrAl materials (APMT and C26M) were like each other and near 0 V NHE. This is not surprising since these last four alloys (X-750, 304SS, APMT and C26M) contain Cr for passivation in high temperature water. That is, the redox processes at the metal surface will “see” chromia in both the austenitic and ferritic alloys. Aluminum or molybdenum do not participate in the passive film [5]. The fact that the proposed FeCrAl cladding will have the same corrosion potential as the grid spacers (e.g. X-750) and other stainless materials (such as the handles of the fuel bundles) will eliminate the occurrence of shadow corrosion in BWR.

At 713 h (30 days, Table 3, Figure 3) of immersion, the purging gas was again changed to hydrogen and the corrosion potential of the six materials returned to the values like in the first period (before 480 h). Based on the corrosion potential data, it is evident that the redox kinetics on FeCrAl is like the well-known behavior of traditional nuclear reactor materials such as type 304SS and X-750 in high temperature water.

TABLE 3. Timeline of the Electrochemical Tests.

Date	Step	Time (days)	Condition
2017 07 19	1	0	Immersion Tests started in pure water 17 MΩ, 288°C, 300 ppb H_2. Monitoring corrosion potential (E_{corr}).
2017 08 08	2	20	Immersion test continues under 288°C pure water and 1000 ppb oxygen. Monitoring E_{corr}.
2017 08 18	3	30	Immersion test continues under 288°C water and 300 ppb H_2. Monitoring E_{corr}.
2017 09 06 to 25	4	31-68	Polarization resistance, pure water, 288°C, 300 ppb H_2.
2017 09 26	5	69	Adding 100 ppm Zn^{2+} as zinc nitrate, conductivity increased ~10,000 times, 288°C, 300 ppb H_2, monitoring E_{corr}.
2017 09 27 to 29	6	70-72	Zinc nitrate effect, polarization resistance and electrochemical impedance spectroscopy (EIS).
2017 11 06	7	73-109	Monitoring E_{corr} in 288°C pure water under 300 ppb H_2 while cleaning the nitrate from the system.
2017 11 06	8	109	Polarization resistance tests in pure water 18 MΩ, 288°C, 300 ppb H_2.
2017 11 06	9	109	Adding 100 ppm Zn^{2+} as zinc acetate, conductivity increased ~10,000 times, 288°C, 300 ppb H_2, monitoring E_{corr}.
2017 11 07	10	110	Polarization resistance and EIS tests to assess effect of zinc acetate addition following by cleaning acetate from the system.
2017 11 17	11	120	System shut down to analyze the specimens.

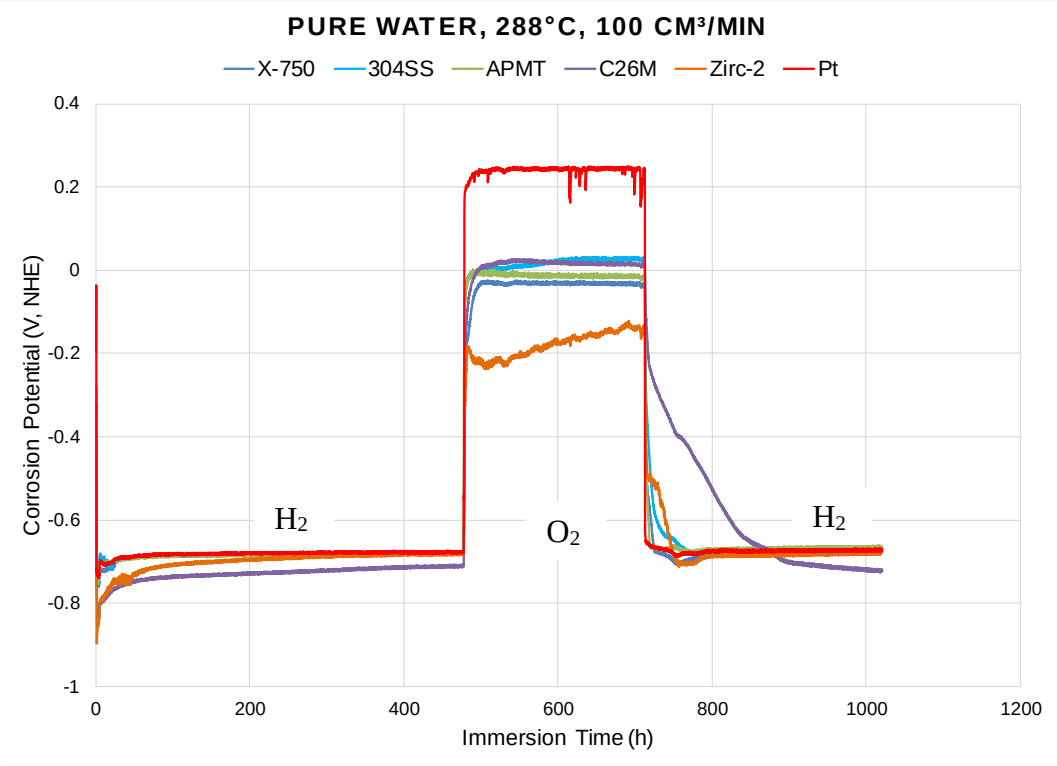

Figure 3. Corrosion potential vs immersion time in pure water at 288°C. In the first and third periods the water contained 0.3 ppm hydrogen and the middle period the water contained 1 ppm dissolved oxygen. Data prove that both C26M and APMT had a similar electrochemical behavior as X-750 and 304SS.

Figure 4 shows the corrosion potential evolution (Step 5 in Table 3) when 100 ppm of Zn^{2+} were added to the circulating water in the form of zinc nitrate ($Zn(NO_3)_2$). Initially (up to 17 h) the system was in presence of 300 ppb H_2, and at hour 17 the zinc nitrate was added. The E_{corr} immediately increased to values above 0 V NHE for all the alloys, even higher than the potential values when the water contained 1000 ppb oxygen (Figure 3). In presence of zinc nitrate the potential values for all the alloys remained high and almost constant suggesting the stability of inorganic nitrate in the system.

Figure 5 shows the E_{corr} evolution (Step 9 in Table 3) when 100 ppm of Zn^{2+} were added to the water in the form of zinc acetate ($Zn(CH_3COO)_2$). As the zinc acetate was added at about 2 h, the potential only increased modestly compared with Figure 4. The potential in presence of zinc acetate only remained modestly higher for a couple of hours, probably due to the decomposition of the organic acetate (Figure 5).

The sequence of impurity (Zn^{2+}) addition in Table 3 was not optimal, it should have been first acetate and then nitrate since acetate affected less the corrosion potential than nitrate. In a near future the effects of zinc addition will be repeated and complemented with results involving mass change coupons of the five alloys in Table 1.

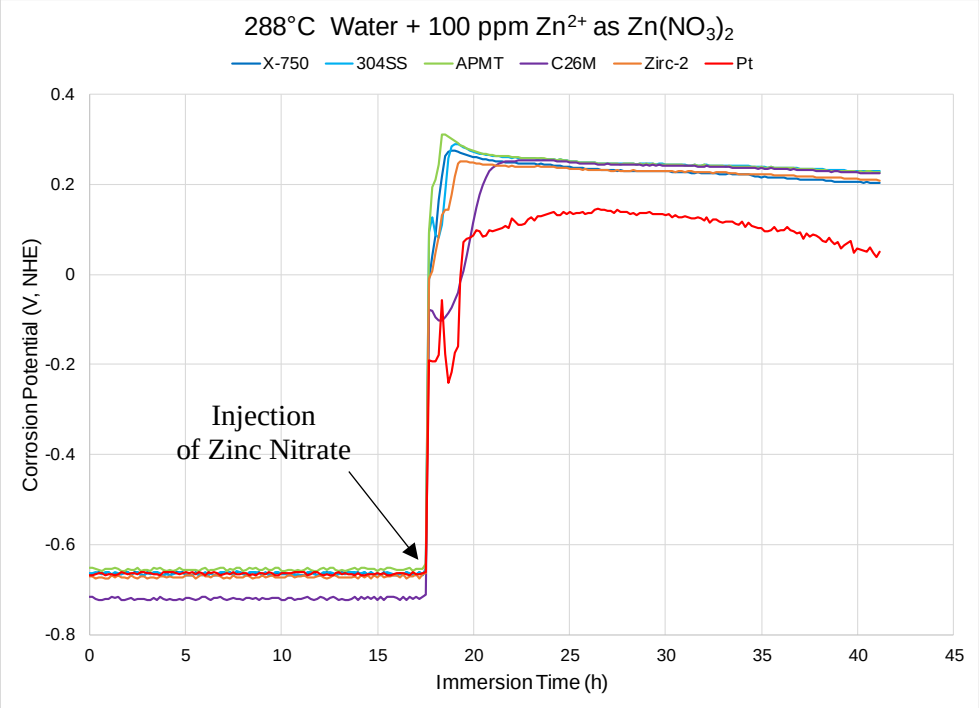

Figure 4. Corrosion potential vs immersion time in water at 288°C. In the first period (up to 17 h) the water contained 0.3 ppm hydrogen and the second period the water also contained 100 ppm of dissolved Zn^{2+} as zinc nitrate. Both C26M and APMT had a similar electrochemical behavior as X-750 and 304SS.

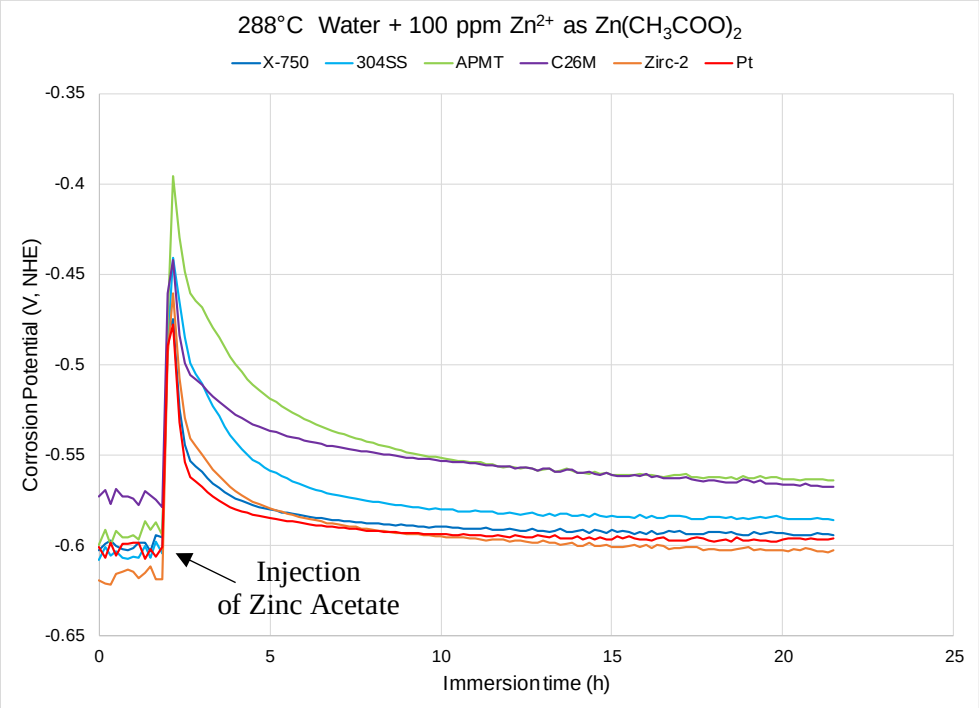

Figure 5. Corrosion potential vs immersion time in pure water at 288°C. In the first period (up to ~2 h) the water contained 0.3 ppm hydrogen and the second period the water also contained 100 ppm of dissolved Zn^{2+} as zinc acetate.

Polarization resistance in 288°C water

Figure 6 shows the polarization resistance R_p (which is inversely proportional to the corrosion rate – Equation 2) for the five tested alloys in hydrogenated pure water. The polarization resistance was approximately 40 kΩ x cm² for the four chromia forming alloys. This shows that ferritic C26M and APMT alloys behave in a similar mode as the traditionally accepted reactor materials X-750 and 304 SS. The polarization resistance value for the Zircaloy-2 specimen was approximately two times the value of the chromia forming alloys.

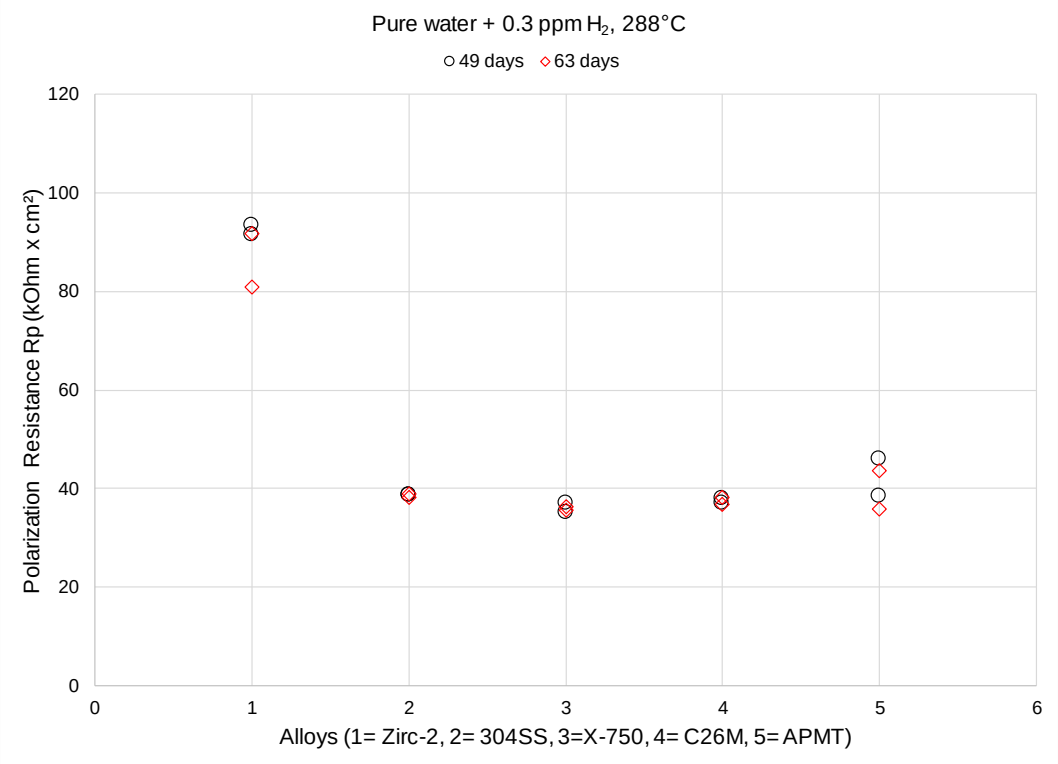

Figure 6. Polarization resistance for the five alloys in pure water containing 300 ppb dissolved hydrogen at 288°C. Both C26M and APMT had a similar resistance to polarization as X-750 and 304SS.

Table 3 shows that at Day 69 zinc nitrate was batch added to the hydrogenated water to make a solution containing 100 ppm of soluble Zn^{2+}. This concentration of zinc is much higher than the traditional plant application of 10 ppb zinc discussed in the introduction. As the water circulated and it was filtered the amount of nitrate and non-deposited zinc gradually decreased. This is not the ideal test (next tests will have a continuous zinc injection for several months in the 5 ppb concentration range). At the nitrate zinc addition, the resistance of the water (electrolyte) dropped from 17 MΩ to approximately 1 MΩ (10,000 times decrease) and the corrosion potential suddenly increased by the presence of the oxidizing nitrate in the water (Figure 4). In two more days the corrosion potential decreased another 400 mV showing the gradual purification of the water. The important fact is that both ferritic alloys C26M and APMT had the same behavior in potential shifts as austenitic type 304SS and X-750 alloys. This is logical since these four alloys form chromia on the surface for corrosion protection at high temperatures.

Figure 7 shows the polarization resistance after the addition of zinc nitrate. The addition of zinc had little or no effect on the behavior of Zircaloy-2 but it affected the resistance to

polarization of the four chromia passivating alloys. This needs to be verified in the near future by using mass change coupons. As stated in the introduction, a true effect of zinc may not manifest itself until after several months of exposure to soluble zinc. Therefore, the data in Figure 7 are for comparative purposes only between C26M / APMT and 304SS / X-750.

After the zinc nitrate addition, the system was conditioned and cleaned by continuous recirculation and filtering of the ions in solution until the water reached again a purity of 18 MΩ at Day 109 (Table 3). Measurements of polarization resistance in purified water Day 109 (Table 3) show that all the five alloys had a similar behavior as in Days 49 & 63 (previous to zinc nitrate injection).

After zinc acetate addition at Day 109 (Table 3 and Figure 5), Figure 8 measurements at Day 110 showed a smaller effect of zinc acetate compared with zinc nitrate. Again, the time of exposure was too short to notice any long term continuous injection for the beneficial effect of zinc. Figures 7 and 8 for short exposure time seem to suggest that Zn would decrease the resistance to corrosion, but this needs to be verified by immersion tests through longer exposure times.

In the current study the effect of zinc injection was performed only in the presence of a hydrogen water chemistry condition. In the next set of tests, the zinc injection will also be studied using a nitrogen or argon conditioned environment.

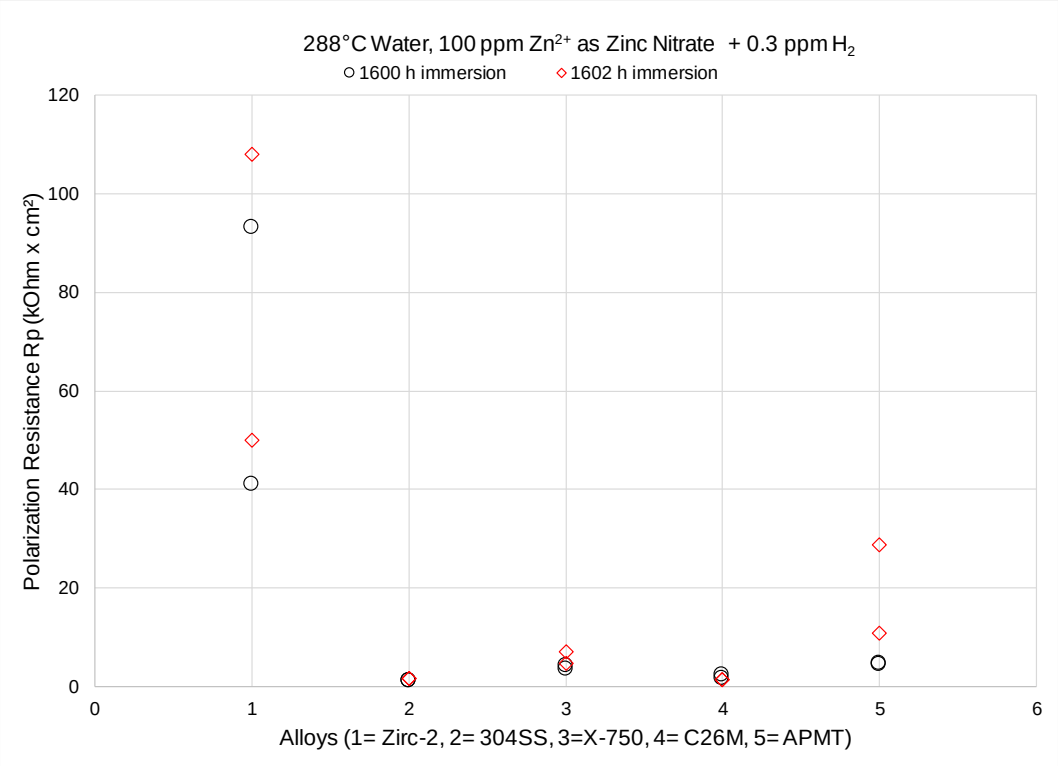

Figure 7. Polarization resistance values for five alloys in pure water containing 300 ppb dissolved hydrogen and 100 ppm Zn^{2+} as zinc nitrate at 288°C. Both C26M and APMT had a similar resistance to polarization as X-750 and 304SS.

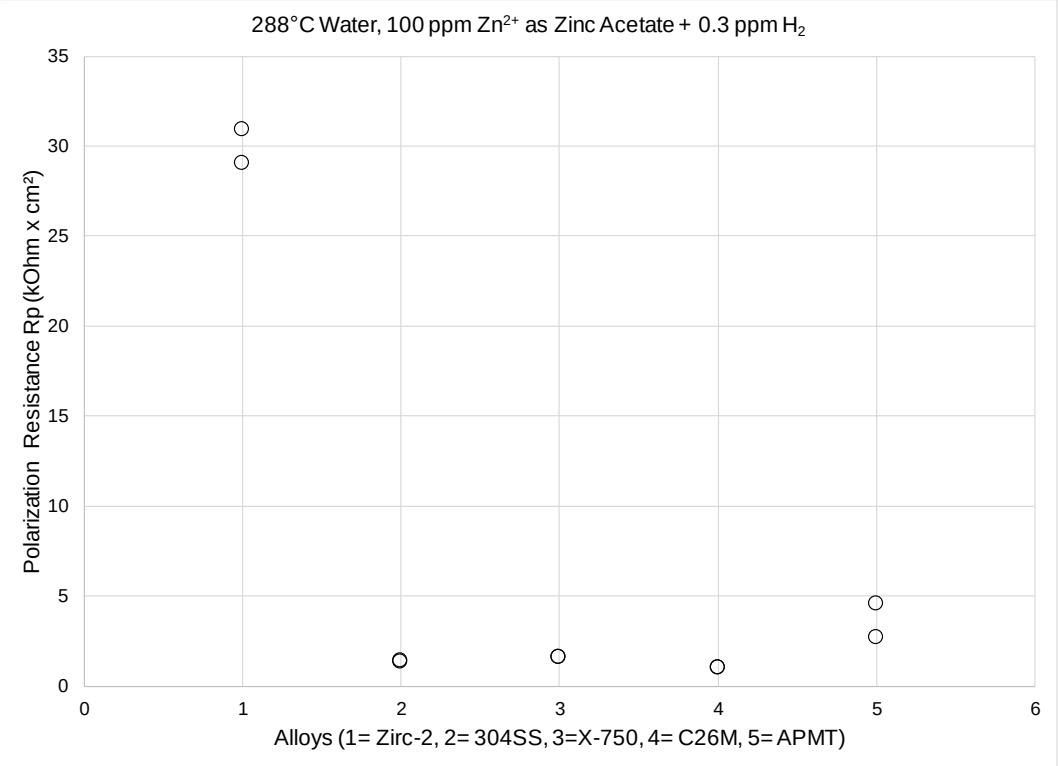

Figure 8. Polarization resistance values for five alloys in pure water containing 300 ppb dissolved hydrogen and 100 ppm Zn^{2+} as zinc acetate at 288°C. Both C26M and APMT had a similar resistance to polarization as X-750 and 304SS.

Preliminary oxide films analyses

Figure 9 shows preliminary examination of the oxide films formed during the 120 days exposure (Table 3) on Zircaloy-2 and APMT. The available data appears to show that zinc did not interact with zirconia on Zircaloy-2 but it may have interacted with chromia on APMT. Next studies will focus in longer time exposure to continuous lower dosages of zinc and comparatives studies of the surface oxides with and without zinc.

Final remarks

Currently and worldwide, most of the cladding for uranium dioxide fuel in light water power reactors is made with zirconium-based alloys. Under severe accident conditions such as the events of March 2011 at the Fukushima site, the zirconium alloys may react rapidly with water and steam forming hydrogen gas that may lead to explosions. It is proposed in several countries that one of the options to resolve this issue is to replace zirconium alloys with FeCrAl ferritic alloys such as APMT or C26M. Since FeCrAl alloys were never used in light water reactors, it is important to characterize their electrochemical behavior in comparison with well tested present reactor alloys, which have been used successfully for over 60 years. Current results show that the corrosion potential of the newer FeCrAl alloys are the same as for those of the common existing materials such as type 304SS or nickel base X-750. That is, by introducing into the reactor the FeCrAl materials, there will be no change in the redox potential system in the reactor environment. It was reported that the type of oxide films that form on FeCrAl alloys in light water reactors environments are like the oxide films that form on austenitic stainless steels or nickel-based alloys containing chromium for passivation [5]. Preliminary short-term studies on zinc addition to the water

show that both C26M and APMT react to the same manner after zinc addition as type 304SS and nickel alloy X-750. That is, the understood beneficial effect of zinc injection into reactors would also benefit the behavior of ferritic FeCrAl alloys. Longer time exposure tests to continuous lower dosages of zinc may confirm the current findings.

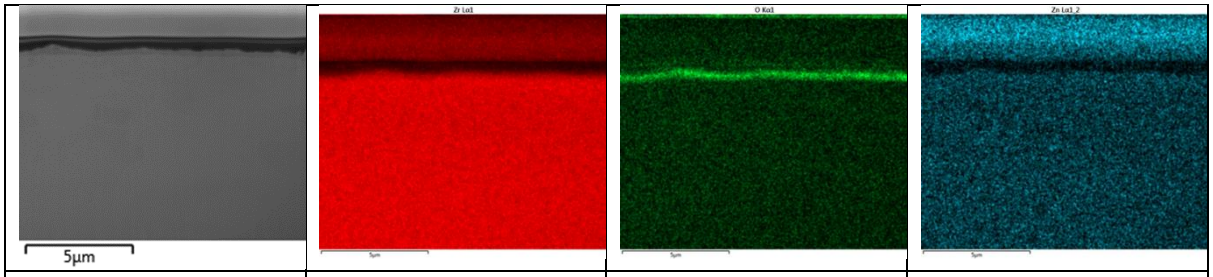

Gray	Zr	O	Zn
Composition of Surface Film for Zircaloy-2			

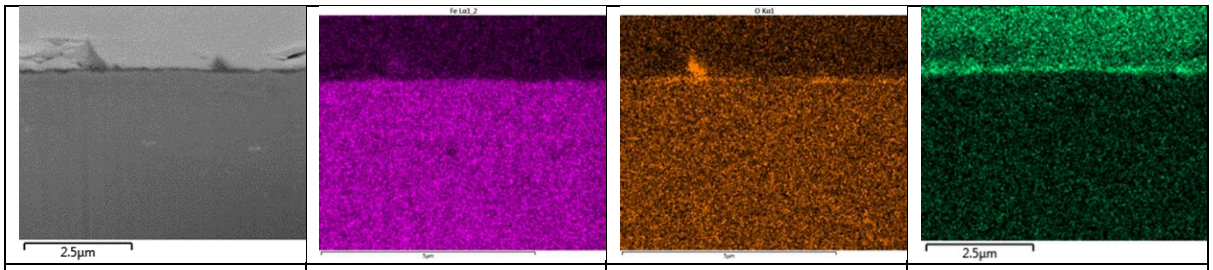

Gray	Fe	O	Zn
Composition of Surface Film for APMT			

Figure 9. Preliminary analysis of surface films after the 120-day immersion tests. There is no apparent interaction between zinc and zirconia but zinc may be incorporating into the oxide protecting APMT.

SUMMARY AND CONCLUSIONS

1) In hydrogenated 288°C water, the corrosion potential of FeCrAl was the same as for the other tested materials such as nickel-based X-750, austenitic stainless steel type 304, Zircaloy-2 and platinum.
2) Under excess oxygen in 288°C water, the corrosion potential of FeCrAl was the same as the corrosion potential of other chromium containing alloys such as type 304SS and X-750.
3) Short term zinc addition studies showed that both C26M & APMT react in the same manner in the presence of soluble zinc as familiar reactor internal alloys 304SS & X-750.
4) The injection of zinc into the high temperature water may affect the corrosion potential of the engineering alloys. Injection of zinc nitrate greatly increased the corrosion potential for longer time while injection of zinc acetate only slightly increased the corrosion potential for shorter time.

ACKNOWLEDGMENTS

This material is based upon work supported by the Dept. of Energy [National Nuclear Security Administration] under Award Number DE-NE0008221. This report was prepared as an account of work sponsored by an agency of the United States Government. Neither the United States Government nor any agency thereof, nor any of their employees makes any warranty, express or implied, or assumes any legal liability or responsibility for the accuracy, completeness, or usefulness of any information, apparatus, product, or process disclosed, or represents that its use would not infringe privately owned rights. Reference herein to any specific commercial product, process or service by trade name, trademark, manufacturer, or otherwise does not necessarily constitute or imply its endorsement, recommendation, or favoring by the United States Government or any agency thereof. The views and opinions of authors expressed herein do not necessarily state or reflect those of the United States Government or any agency thereof.

REFERENCES

1. K. A. Terrani, “Accident Tolerant Fuel Cladding Development: Promise, Status, and Challenges,” *JNM*, 10.1016/j.jnucmat.2017.12.043, American Nuclear Society (2018)
2. R. B. Rebak, “Iron-chrome-aluminum alloy cladding for increasing safety in nuclear power plants, EPJ, Nuclear Sci. Technol. 3, 34 (2017).
3. S. M. Bragg-Sitton (2016), M. Todosow, R. Montgomery, C. R. Stanek, R. Montgomery, and W. J. Carmack, Metrics for the Technical Performance Evaluation of Light Water Reactor Accident Tolerant Fuel, Nuclear Technology, 195(2), p. 111-123, August 2016.
4. R. E. Stachowski, R. Fawcett, R. B. Rebak, W. P. Gassmann J. B. Williams, K. A. Terrani, “Progress of GE Development of Accident Tolerant Fuel FeCrAl Cladding” Paper A-287, WRFPM 2017, Jeju-do, Republic of Korea, September 2017.
5. R. B. Rebak, “Versatile Oxide Films Protect FeCrAl Alloys Under Normal Operation and Accident Conditions in Light Water Power Reactors,” *JOM*., (2018) 70: 176. https://doi.org/10.1007/s11837-017-2705-z.
6. D. Perkins, K. Ahluwalia, J. Deshon, C. Haas, An EPRI perspective and overview of PWR Zinc injection, in: Proceedings of International Conference on Water Chemistry of Nuclear Reactor Systems, VGB, Berlin, 2008, paper P2-26.
7. S.E. Ziemniak, M. Hanson, Zinc treatment effects on corrosion behavior of 304 stainless steel in high temperature, hydrogenated water, Corros. Sci. 48 (2006) 2525–2546.
8. Overview Report on Zinc Addition in PWRs, EPRI, Palo Alto, CA: 2001: 1001020.
9. T.M. Angeliu, P.L. Andresen, Effect of zinc additions on oxide rupture strain and repassivation kinetics of iron-based alloys in 288 °C water, Corrosion 52 (1996) 28-35.
10. I. Betova, M. Bojinov, P. Kinnunen, and T. Saario, “Zn injection in Pressurized Water Reactors – laboratory tests, field experience and modelling,” Research Report VTT-R-05511-11 (2011).